View metadata, citation and similar papers at core.ac.uk
brought to you by CORE
provided by Edinburgh Research Explorer

JASs Invited Reviews
Journal of Anthropological Sciences
Vol. 87 (2009), pp. 127-151

Measurement of brain volume using MRI: software, techniques, choices and prerequisites

Simon S. Keller[1] & Neil Roberts[2]

1) Clinical Research Imaging Centre (CRIC), Queen's Medical Research Institute (QMRI) University of Edinburgh
e-mail: kellers@liv.ac.uk

2) Division of Medical and Radiological Sciences, School of Clinical Sciences and Community Health, University of Edinburgh, UK

Summary - *Magnetic resonance imaging (MRI) permits in vivo quantification of brain compartment volume, and has many applications in cognitive, clinical and comparative neuroscience. There are numerous approaches for obtaining a brain volume estimate from MRI, and the primary focus of this paper is to provide an overview of the methods available to estimate the volume of three brain structures that are of particular interest in the neurosciences: the cerebral hemispheres, hippocampus and Broca's area. We provide information on choice of computer software, hardware compatibility, required user expertise, the application of manual and automated MR image analysis techniques, and anatomical guidelines, providing the reader with enough information to decide on their approach at the outset of a quantitative MRI study. We advocate the use of stereology in conjunction with point counting for an unbiased and time efficient estimate of brain compartment volume.*

Keywords - *Image Analysis, Broca's Area, Cerebral Hemisphere, Hippocampus, Stereology.*

Introduction

Magnetic resonance imaging (MRI) has become the method of choice for the examination of macroscopic neuroanatomy in vivo due to excellent levels of image resolution and between-tissue contrast. A wide variety of software packages are available for viewing and appraising MR images, for reformatting the images in three dimensions so as to obtain sections with a particular orientation through the body and for making both simple and more sophisticated measurements of regions of interest, compartments and individual structures. This paper is concerned with measurement of brain volume. On the one hand the MR system manufacturer may provide a suite of tools on the MR system console that enable the clinician, for example, the Radiologist, to supplement their diagnostic report with objective data, the MR Physicist or Radiographer to carry out relevant quality assurance programmes, or the Researcher to obtain simple measurements of, for example, image signal intensity, size, etc (e.g. the Leonardo Workstation sold by Siemens Medical Systems, see 'Info on the Web' Section of this manuscript). Furthermore, a third party company with a specific interest in topics such as, for example, radiotherapy planning, functional brain imaging (e.g. BrainVoyager, see 'Info on the Web' Section), image analysis (e.g. Quantificare, see 'Info on the Web' Section), etc. will offer for sale a product that allows the practitioner or scientist to input the relevant MR images and perform more sophisticated expert analyses. On the other hand (and where measurements are most often made) a University or

Government Funded Research Department may develop a library of image processing algorithms or measurement techniques (e.g. Statistical Parametric Mapping (SPM)) for the purpose of answering specific scientific questions, that are not offered immediately as a product, but eventually may be set within a more convenient user interface and offered as product through a third party (e.g. SPM within BrainVoyager). Examples of University Departments with a specific scientific focus are The Wellcome Functional Imaging Laboratory (www.fil.ion.ucl.ac.uk) concerned with Human Brain Mapping, and INRIA (www.inria.fr) concerned with tissue characterisation and image registration.

In this paper we describe the application of quantitative image analysis techniques to obtain a brain volume estimate from MR images. Our main focus is to describe the application of stereological methods for the analysis of MR images as has been pioneered at, for example, the Research Laboratory for Stereology, University of Aarhus, Denmark, the Stereology Unit, University of Santander, Spain, and the Magnetic Resonance and Image Analysis Research Centre (MARIARC), University of Liverpool, UK. Stereology is defined as the statistical analysis of geometric parameters from sampled information. In other words, such quantities as the volume of the brain (e.g. Keller *et al.,* 2002a, 2002b, 2007c; Roberts *et al.,* 2000), the surface area of the cerebral cortex (e.g., Roberts *et al.,* 2000; Ronan *et al.,* 2006, 2007) and the length of the cerebral arteries (e.g., Roberts *et al.,* 1991) may be estimated without sampling bias and with known precision. Typically, stereological methods are applied manually in two stages. Firstly, appropriate two-dimensional (2D) sections or projections of the structure of interest must be obtained either directly at the time of imaging or indirectly by appropriate reformatting of acquired three-dimensional (3D) data sets. Although the methods are manual they are extremely efficient and before any major project is undertaken, a pilot study can be usefully undertaken to define an exact sampling design that will optimise the workload for that particular project (see, for example, Garcia-Finana and Cruz-Orive (2000) in the case of brain research). The software package EASYMEASURE was developed at MARIARC (see Keller *et al.*, 2007c) to enable convenient application of stereological methods to MR images via the use of digital sampling probes (i.e. test points and cycloid test lines). Other software that permit similar analyses are MEASURE software (Barta *et al.* , 1997) and the computer assisted stereological toolbox (CAST) software (www.olympusamerica.com/microscopes). Previously, our paper published in The British Journal of Radiology (Roberts *et al.,* 2000) aimed at helping Radiologists to consider applying stereological methods for the analysis of the volume and surface area in routine clinical diagnosis. In the present paper we address only volume estimation and our goal is to assist Neuroscientists from a wide range of backgrounds (e.g. cognitive neuroscience, clinical neuroscience, comparative neuroscience, anthropology) to consider applying stereological methods for the analysis of the volumes of individual brain structure and compartments using MRI.

Furthermore, so as to be both complete and comprehensive we present a detailed and illustrated exposition of the three main scenarios that may be encountered. In particular, firstly, we consider the case of obtaining the volume of a relatively well-isolated structure of interest, in this case the whole cerebral hemisphere. Applications of this may be in the study of individual brain structures (e.g. amygdala in psychiatric studies, lateral ventricles in dementia studies) or to normalise individual brain structure estimates. Secondly, we consider the estimation of the volume of a brain structure that is not so well isolated, namely the hippocampus. This structure is of particular interest in that it may be routinely estimated in a medical setting in the context of pre-surgical evaluation in patients with clinical evidence of temporal lobe epilepsy. A strategy needs to be developed for defining the posterior boundary of the hippocampus so as to separate it from adjacent tissue. Thirdly, we consider the estimation of the volume of a structure that is not at all well isolated, and yet frequently measured and

of major scientific interest and curiosity, namely Broca's area. We review the approaches that have been used and report on a technique we developed at MARIARC, University of Liverpool, UK and which we are most recently using in collaboration with the Yerkes Primate Research Centre, Atlanta, USA (www.yerkes.emory.edu/) in a comparative study of differences in the so-called language circuit between humans and primates. The three structures of interest are indicated in Figure 1. Throughout the manuscript we place particular emphasis on technical specifications and the human expertise required to obtain a volume estimate for each structure.

Acquisition of the MR Image

Estimation of brain compartment volume requires high resolution MR images for the delineation of anatomical boundaries. The most frequently used MR scanners are either 1.5 Tesla (T) or 3 T systems. Both systems permit quantification of global and regional brain structure. Although 3 T systems offer increased resolution of between-tissue contrast (i.e. increased visualisation of the borders between grey matter, white matter and cerebrospinal fluid (CSF)), MR scans on 1.5 T systems are sufficient for the quantification of relatively small brain structures, such as the hippocampus, amygdala, and deep grey matter nuclei (e.g. basal ganglia). The type of MR sequence used for the application of quantitative MR image analysis however is a more important consideration for volume estimation.

There are several types of MR sequences available for structural neuroimaging, most commonly T1-weighted, T2-weighted and Proton Density imaging. The differences in image contrast are due to the differences in relaxation properties of hydrogen nuclei between tissue types. Depending on how the sequence parameters are programmed, each sequence can be either 2D or 3D, and most quantitative techniques utilise 3D sequences. T1-weighted imaging (Fig. 2) offers the greatest clarity between grey matter, white matter and CSF, and is therefore most frequently used for quantitative MRI studies of brain morphology, particularly of individual brain structures. On the other hand, T2-weighted imaging (Fig. 2) may be preferably used for quantification of intracranial volume, given that the increased signal intensity of CSF in this sequence permits easier quantification of CSF and brain parenchyma together. There are many types of T1-weighted sequences, each having associated

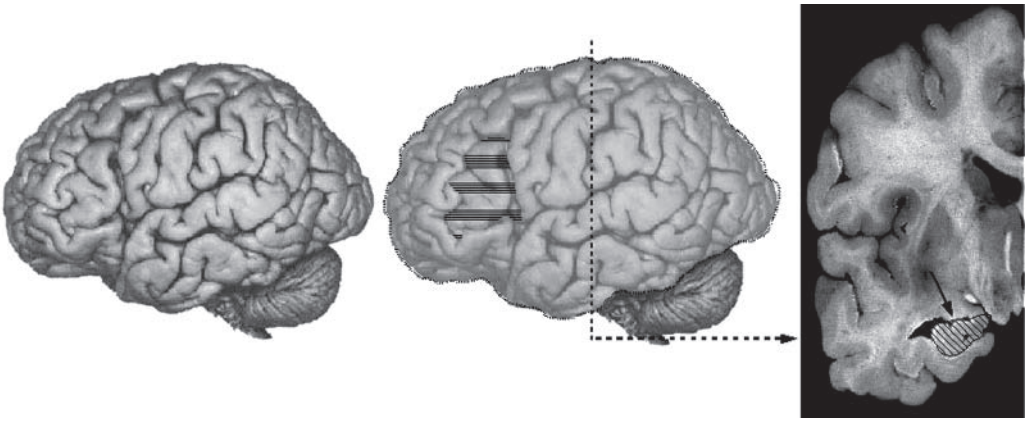

Fig. 1 - Location of the three brain regions described in this paper. Left: Lateral view of a post-mortem brain specimen. Middle: Cerebral hemisphere (transparent grey / broken black outline) and Broca's area (hatched lines) of the post-mortem brain. Right: Hippocampus (outlined region / arrow) in the medial temporal lobe. The dashed vertical line indicates the approximate location of the coronal view on the right.

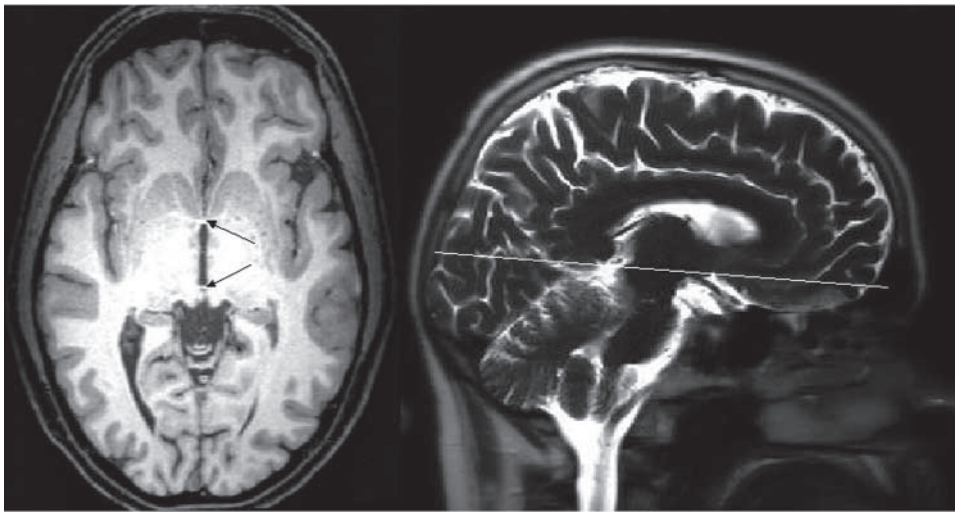

Fig. 2 - T1-weighted axial (left) and T2-weighted sagittal (right) MR images of a human brain. The approximate location of the axial section is indicated by the white line on the sagittal image. Arrows indicate the anterior and posterior commissure on the axial image: this image has been realigned orthogonal to the bicommissural plane.

advantages. For example, a high-resolution 3T MPRAGE sequence generally offers excellent between-tissue clarity, particularly of the cortical ribbon, and clear visualisation of small structures, such as the alveus in the medial temporal lobe. However, there are some drawbacks to the use of this sequence, particularly the lack of tissue differentiation around the thalamic area (which is always a problem for structural MR imaging) and signal drop out in the ventral temporal lobes altering the morphology of the fusiform gyrus in particular. The MDEFT T1-weighted sequence (Deichmann *et al.,* 2004) overcomes signal drop out in the ventral temporal lobes, but offers reduced grey matter-white matter clarity where these tissues meet in neocortical areas.

Quantitative Analysis of MR Images

Laboratory Set-Up

The primary prerequisite for a quantitative MR image analysis laboratory is one or several computers with capabilities for high demand processing, although the extent of processing power depends on the software utilised and the requirements of the planned investigation. For example, a simple volume estimation of individual brain structures using manual methods such as stereology or tracing (see below) may require up to 1 gigabyte (GB) of Random Access Memory (RAM). Alternatively, automated tissue classification (e.g., grey matter, white matter, CSF) and cortical reconstruction (see below) may require at least 8 GB of RAM. Furthermore, given that a single MR image can range from 4 megabytes (MB) to over 100 MB in size, it is important to have a computer with enough storage space for hundreds and perhaps thousands of images, particularly for studies using automated methods that generate multiple reformatted, MR image inhomogeneity corrected, spatially processed, segmented and reconstructed images from a single raw MR image. Moreover, several software packages are not compatible with all platforms, although all are compatible with Windows, Linux, Macintosh or SUN systems. Research groups should therefore prospectively consider software-hardware compatibility issues in light of the quantitative techniques to be used.

Techniques

There is a plethora of techniques available to estimate brain compartment volume from MR images. This section describes some methodological fundamentals for some image analysis techniques, indicating the type of analyses permitted and the requirements for the various techniques. The simplest way to describe MRI quantitative methods is to classify according to manual or automated approaches. Manual methods require investigator expertise to delineate gross neuroanatomical boundaries (for example, sulcal contours or subcortical landmarks) whilst automated methods largely remove the need for an anatomist and rely on computerised techniques to extract information on brain morphology.

Manual techniques

Prior to manual analyses, it is important to align all participants' MR images into a standard orientation. There are several ways in which this can be performed, and there are multiple orientations to standardise to, the choice of orientation should be determined by particular research agendas. Image realigment can be performed using a variety of techniques and software packages (see below). Some software packages permit automated realignment into a standard stereotaxic system by spatially normalising images to correct for gross differences in brain shape, size and skew. These automated methods register the target MR image to a template image typically constructed from a representative population of MR subjects (i.e. a group mean image). Images can also be manually realigned. The most common orientation used for MR-based volumetry is generally orthogonal to the bicommissural plane whereby the image is rotated and interpolated until the anterior commissure and posterior commissure can be visualised on the same axial section (ordinarily with additional edits to correct brain skew, Fig. 2). However, images can be realigned orthogonal to other anatomical planes depending on the structure to be measured, for example, the long axis of the hippocampus for hippocampal measurements, or orthogonal to the greatest length of the Sylvian fissure for measurements of the planum temporal (a cortical area within the superior temporal gyrus, which is located posterior to Heschl's gyrus).

Manual techniques require the investigator to delineate a brain region based on reliable anatomical landmarks, whilst the software package provides information on volume (or other variables of interest, such as surface area or cortical thickness of the delineated structure). There are two primary methods for manual quantification of brain compartment volume from MR images, namely stereology in conjunction with point counting and tracing methods.

Stereological methods have been widely applied on MR images to estimate geometric variables, such as volume and surface area, of internal brain compartments. Detailed explanations of the application of stereological methods to obtain volume estimates can be found in our previous studies (García-Fiñana *et al.,* 2003, 2009; Roberts *et al.,* 2000). We have previously applied this technique to obtain volume estimations of various brain structures, including hippocampus, temporal lobe, Broca's area, prefrontal cortex and cerebral hemisphere (Cowell *et al.,* 2007; García-Fiñana *et al.,* 2003, 2006; Keller *et al.,* 2002a, 2002b, 2007b, 2007c). In these studies, a set of parallel and equidistant MR images of the brain is randomly selected, and the area of interest is directly estimated on each image by randomly superimposing a grid of points, and subsequently, counting the number of points that fall within the region of interest. The mathematical justification and implementation of this method is simple, although how to predict its precision is a complex problem due to the spatial dependence of the observations, and for this reason, it has been a constant subject of discussion among statisticians (García-Fiñana *et al.,* 2009). One important benefit of stereology in combination with point counting is with respect to the time taken to estimate volume of brain structures on MR images, which is much more time efficient than manual tracing or segmentation methods which are extremely labour intensive (Doherty *et al.,* 2000; Gong *et al.,* 1999; Sheline *et al.,* 1996). Moreover, stereology

permits the prediction of the coefficient of error, which provides information on how precise volume estimations are. The coefficient of error can also be used in preliminary analyses to identify the optimal parameters of sampling needed to achieve a given precision (for example, the number of MR sections and the density of the point grid).

Rather than counting the number of points within the structure transect area as per stereological methods, tracing methods require the investigator to trace the brain region of interest using a mouse driven cursor throughout a defined number of MR sections. The transect areas, determined by pixel counting within the traced region, are summed and multiplied by the distance between the consecutive sections traced to estimate the volume. Whilst tracing methods represent the most commonly used tool to estimate brain structure volume on MR images (for example, see Geuze *et al.,* 2005), there are some drawbacks associated this technique. Firstly, the time taken to perform manual tracing or manual segmentation methods is significantly longer than stereological point counting methods. Secondly, tracing and manual segmentation methods suffer from the risk of 'hand wobble' during the continuous delineation of region of interest boundaries on MR sections, which may cause the exclusion of legitimate or inclusion of illegitimate brain tissue. This is not the case with point counting methods which require the rater to remove or mark the number of points intersecting the region of interest.

All manual region of interest quantitative methods require observer expertise in gross neuroanatomy, and it is for this reason that these methods are considered the most reliable methods for obtaining volume estimates relative to automated techniques. It is therefore crucial that the investigator undergoes thorough training for quantitative analysis using intra- and inter-rater studies before any study is started to confirm that he or she can reproduce the same measurement. Intra-rater analyses require the observer to estimate the volume, surface area or other variable of interest from the same MR images more than once, preferably some weeks apart, blinded to subject identification, to confirm that he or she can reproduce the same measurement as they previously did. Inter-rater analyses require a blinded comparison between two or more observers to confirm reliability.

Automated techniques

Unlike manual quantitative region of interest methods, semi-automated and automated methods do not require manual delineation of brain structures through a determined number MR sections. Usually, semi-automated methods require manual marking of some anatomical landmarks, which is followed by an automatic segmentation of the region of interest based on the position of the landmarks and image intensity thresholds. Automated methods are entirely user-independent and may utilise geometric template matching methods to extract brain size and shape parameters. The primary drawback of semi-automated and automated techniques is lack of anatomical specificity generated; manual techniques require experienced raters with detailed knowledge of neuroanatomy, and estimates can be confidently ascribed to the neuroanatomical region of interest. On the other hand, manual techniques have practical drawbacks including increased labour intensity and reduced time efficiency.

The past decade has seen a proliferation of computerised automated processes that enable user-independent spatial normalisation, segmentation and cortical reconstruction of MR images (Fig. 3). A vast number of reports exist on the development of automated image analysis procedures (e.g. Toga & Mazziotta, 2002). However these methods share some common features, such as various geometric parameters with reference to a stereotaxic template for spatial normalisation, and either a combination of between-tissue signal intensity differences and reference to a stereotaxic template or just signal intensity differences for segmentation of grey matter, white matter and CSF. These spatial transformations enable cohort comparisons given that homologous brain regions can be compared between brains, or between hemispheres in analyses of

cerebral asymmetry. Reconstruction of the cortical surface can also be obtained based on the segmentation of grey matter and white matter. These methods have a variety of applications, including the visualisation of normal and diseased surface brain anatomy, estimation of cortical volume and surface area, and localisation of neural activity for functional MRI studies.

Automated registration and tissue classification enable quantitative comparisons of brain morphology between cohorts of subjects. Voxel-based morphometry (VBM) (Ashburner & Friston, 2000) is a fully automated user-independent MR image analysis technique that permits voxel-wise statistical comparisons over the entire brain providing information about regional brain concentration or volume differences between cohorts of subjects. Voxel-wise parametric statistics are used to compare the morphology of homologous brain regions on MR images that have been spatially normalised into a common stereotaxic space, tissue-classified (grey matter, white matter and CSF) and smoothed using an isotropic Gaussian kernel. Given that the technique is fully automated and therefore time efficient, there has been a proliferation of VBM studies in patient and neurologically healthy populations over the past decade. Several studies have attempted to demonstrate the methodological validity of VBM by comparing it with manual region of interest techniques (Good *et al.,* 2002; Keller *et al.,* 2002a, 2002b), by investigating the optimal normalisation, segmentation and smoothing combinations (Keller *et al.,* 2004; Wilke *et al.,* 2003) and in comparison with functional neuroimaging methods (Keller *et al.,* 2007a). However, VBM has many methodological limitations, all of which should be fully considered prior to starting a study (Ashburner & Friston, 2001; Bookstein, 2001; Keller and Roberts, 2008). In particular, we have previously discussed how VBM cannot be applied to infer changes in anatomy based on individual MRIs (compared to group comparison studies), should not be used to assess white matter changes based on T1-weighted images, does not have the capacity to identify brain abnormalities that are not shared by the vast majority of a patient population, and how results may differ according to various approaches made by the investigator (e.g. different statistical thresholds, different spatial normalisation parameters, different smoothing kernel sizes) (Keller & Roberts, 2008).

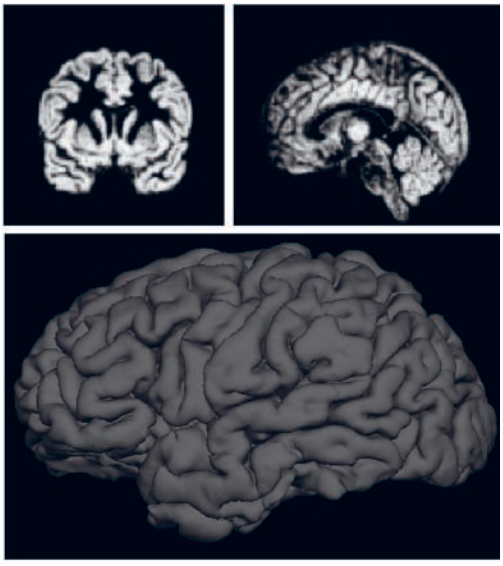

Fig. 3 - Examples of automated spatial processing of MR images. Top: Coronal (left) and sagittal (right) illustration of an MR image that has been automatically spatially normalised into a stereotaxic bicommissural system and grey matter automatically segmented using SPM software. Bottom: 3D cortical reconstruction of an MR image with removal of the cerebellum and brainstem using FREESURFER software.

Software

There are many software packages available for quantitative image analysis. Many of these packages have evolved from earlier versions, ordinarily based on mathematical modifications to ensure improved geometric transformations during automated analyses. The vast majority of software packages are free to download from Internet sites from host institutions that developed the packages. We present some of the most frequently used software packages for quantitative MRI of the brain in

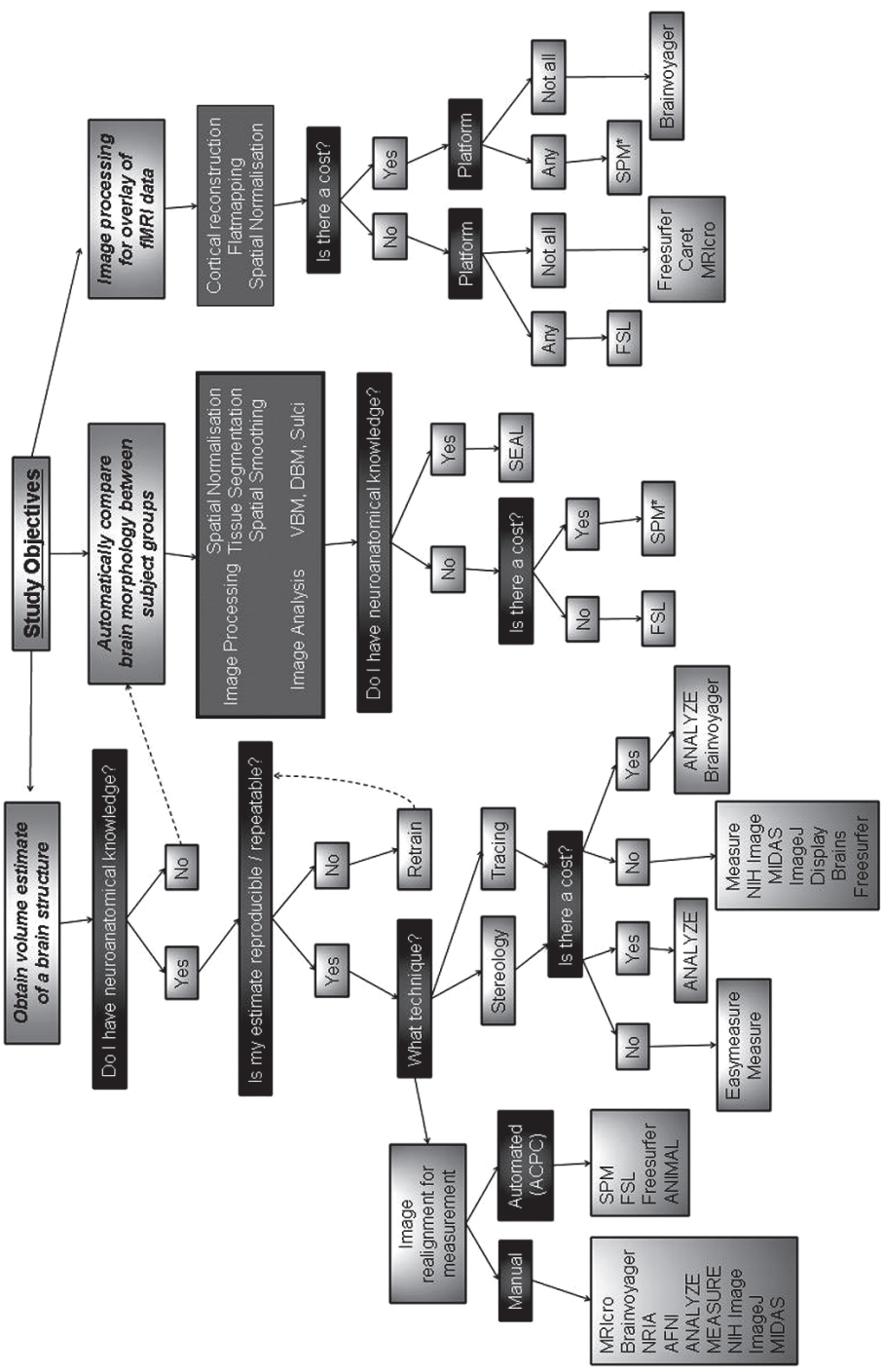

Fig. 4 - A flow diagram of some of the basic choices an investigator is faced with when planning a quantitative MRI study, with particular reference to the choice of software. Please refer to the Appendix for more information on each software package. *The cost to run SPM pertains to a Matlab licence and not SPM itself. DBM, Deformation-Based Morphometry; VBM, Voxel-Based Morphometry (Ashburner and Friston, 2000).

the Appendix and Fig. 4. Figure 4 presents a flow diagram of some of the basic choices an investigator faces when planning a quantitative MRI study, with particular reference to the choice of software. More detailed information for each software package is provided in the Appendix and the references therein. We provide as much information as possible for each software package, including appropriate references to obtain the software, software and hardware compatibility issues, software cost, software functions, and required user expertise. It is important to note that the features described in the Appendix and Figure 4 are not the only features offered by each software package, and represent the features familiar to the authors of the present manuscript. We recommend that the websites provided are visited and / or authors of each paper contacted for further information.

Quantitative MRI in practice

Drawing on the above information, we provide basic descriptions of how to estimate the volume of three brain structures using a variety of techniques and software packages. We remind the reader that these methods do not represent the full repertoire of techniques available, but allow us to demonstrate how to measure the three structures using alternative methods. For each structure, we begin by describing the anatomy to be quantified, with discussion of contentious landmarks where appropriate, before demonstrating the application of some techniques to obtain a volume estimate.

Cerebral hemispheres

The cerebral hemispheres are typically described as including all supratentorial grey matter and white matter, excluding brainstem and cerebellum (e.g. Barrick *et al.,* 2005; Cowell *et al.,* 2007).

There are several methods that enable volume estimation of the cerebral hemispheres including stereological (Cowell *et al.,* 2007; Mackay *et al.,* 1998), semi-automated (Filipek *et al.,* 1994; Sisodiya *et al.,* 1996) and automated (Barrick *et al.,* 2005) techniques, some of which are illustrated in Figure 5. Tracing methods are now rarely used to estimate the volume of the cerebral hemispheres given the extensive amount of time and investigator labour required to manually outline the convolutions of the hemispheres on multiple sections. The fully automated method described by Barrick *et al.* (2005) requires the raw MR image to be skull stripped (i.e. removal of skull from brain) and tissue classified (i.e. grey matter / white matter / CSF) using SPM or FSL, and supratentorial hemispheric extraction using the method of Maes *et al.* (1999). This method allows all images within a study to be batch-processed, so that once the investigator chooses the image files for segmentation and extraction, there is no further investigator involvement until all image processing is complete. In contrast, the stereological method requires continuous investigator-computer interaction as all points intersecting the cerebral hemispheres are removed or marked on consecutive evenly spaced MR sections. For each brain structure measured using stereology in conjunction with point counting, the stereological parameters (grid size, slice gap) need to be optimized so that each measurement is reliable (as assessed by the coefficient of error associated with the volume estimate) and is time efficient. In other words, enough points need to be counted (ordinarily at least 200 per structure) so that the estimate is reliable, but not too many points as this will result in decreased time efficiency. For the cerebral hemispheres, previous work has shown that a grid size of 15 and slice gap of every 15 sections results in approximately 200 points being counted per hemisphere on frequently acquired 3D T1-weighted images (e.g. Mackay *et al.,* 1998; Cowell *et al.,* 2007), and achieves a coefficient of error lower than the optimal 5% (Roberts *et al.,* 2000). Stereological volume estimation of a cerebral hemisphere using the Windows-based software packages (EASYMEASURE and MEASURE) takes approximately 10 minutes.

A frequently used method to obtain an automated volume estimation of the whole brain is based on the tissue segmentation algorithms of SPM or FSL. A simple estimation of brain size

can be obtained by automated pixel counting of the grey matter and white matter images to give a total brain volume. However, this method does not parcellate the supratenorial hemispheres and includes both brainstem and cerebellum, and is more an estimation of intra-cranial volume than cerebral hemisphere volume. This method is also shown in Figure 5.

Hippocampus

A large volume of literature surrounds the development of techniques to accurately and reliably measure the hippocampus. This is due to a combination of factors such as: (a) high clinical and scientific interest; and (b) measurement difficulties linked to the small size and anatomical complexity of the hippocampal formation.

Despite the publication of core textbooks detailing hippocampal anatomy frequently referred to in MRI studies of hippocampal volume (for example, Duvernoy, 1998), the boundary definitions used between many studies differ. The various anatomical landmarks used to demarcate hippocampus from adjacent tissue are likely to have a significant effect upon volume estimations and reliability measures. If not all, the vast majority of studies estimating hippocampal volume include the hippocampus proper (Ammon's horn), dentate gyrus, and usually the subiculum. These structures comprise the 'hippocampal formation' and are almost visually indistinguishable on standard MR images, and are therefore usually sampled as a whole complex (Pantel *et al.,* 2000). Some studies have additionally included small

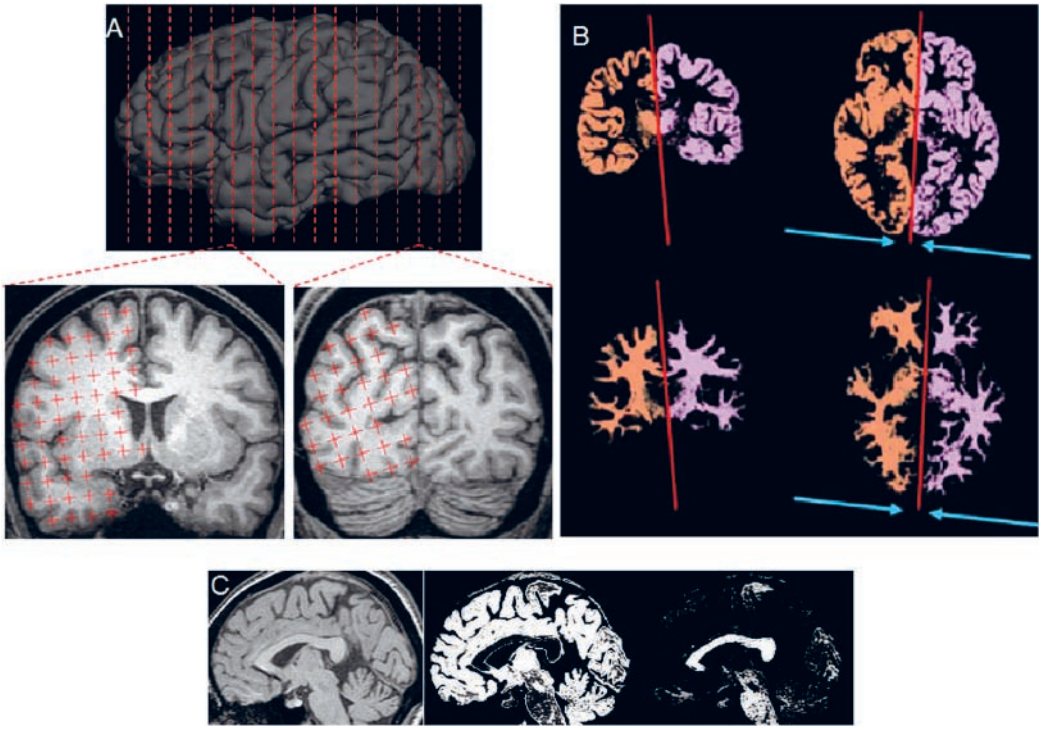

Fig. 5 - Methods to estimate the volume of cerebral hemispheres. A. Stereology in conjunction with point counting. Equally spaced MR sections are sampled using point counting techniques. B. Automatic cerebral hemisphere extraction and volume estimation using the method of Barrick et al. (2005). C. Volume estimation of automatically segmented grey matter (middle) and white matter (right) compartments using SPM software.
The colour version of this figure is available at the JASs website.

white matter structures like the alveus and fimbria (Cook *et al.,* 1992; Jack *et al.,* 1989; Keller *et al.,* 2002a; Mackay *et al.,* 1998; Pruessner *et al.,* 2000; Salmenpera *et al.,* 2005), whilst others have not (Hogan *et al.,* 2000b; Hogan *et al.,* 2004; Pantel *et al.,* 2000). Some studies have included the uncus and choroid plexus (Ashtari *et al.,* 1991; Cook *et al.,* 1992). However, the factors that are most likely to have an effect on volume estimation between studies are the anterior and posterior limits of the hippocampal region of interest.

Typically, the anterior-most regions of the hippocampus are differentiated from the adjoining amygdala by visualisation of the alveus, which is clearly seen on high-resolution MR images. The alveus is the prevailing anterior boundary for hippocampal volume measurements (Geuze *et al.,* 2005) and represents an anatomically correct demarcation. Other studies have used arbitrary extrahippocampal landmarks for demarcation of the anterior border of the hippocampus when lower resolution MR images have been obtained, such as the mammillary body and the superior choroidal fissure (Jacobsen *et al.,* 1996; Lencz *et al.,* 1992; Shenton *et al.,* 1992). Considering that the anterior portions of the hippocampus are preferentially affected in at least some neurological disorders (Woermann *et al.,* 1998) and preferentially related to particular aspects of cognition (Hackert *et al.,* 2002) relative to more posterior hippocampal regions, it is crucial that volumetric measurements sample the entire hippocampal head, using the alveus as the anterior border, as visualised using all three (coronal, axial and sagittal) orthogonal MR sections.

Given the ambiguity associated with demarcation of the hippocampal tail from adjacent tissue, most studies have chosen an arbitrary extrahippocampal landmark for the posterior limit of the hippocampus. The posterior-most section of the hippocampus is most commonly the section where the crus of the fornix is visualised in its full profile (Cook *et al.,* 1992; Watson *et al.,* 1992). Other posterior landmarks include the section i) on which the lateral ventricles divide into frontal and temporal horns (Keller *et al.,* 2002a; Lim *et al.,* 1990; Mackay *et al.,* 1998; Zipursky *et al.,* 1994), ii) on which the pulvinar of the thalamus is seen in full profile (Theodore *et al.,* 1999; Theodore and Gaillard, 1999; Theodore *et al.,* 2001), iii) on which the mammillary bodies are seen in full profile (Becker *et al.,* 1996), iv) 3mm anterior to the superior colliculi (Spencer *et al.,* 1993), v) 3mm anterior to ascending portion of hippocampal tail (Marsh *et al.,* 1997), vi) showing bifurcation of the basilar artery (Bremner *et al.,* 1995), vii) showing the posterior commissure (Jack *et al.,* 1989), viii) showing the merging of the superior colliculus and thalamus bilaterally (Brambilla *et al.,* 2003) and ix) at which the internal auditory canal appears (Reiss *et al.,* 1994). Some studies have measured the whole hippocampus without sacrificing any of the hippocampal tail (Hogan *et al.,* 2000, 2004; Pruessner *et al.,* 2000), which is most reliably achieved using a combination of excellent tissue contrast and orthogonal sections for measurements.

MRI-based definitions of circumscribed brain regions require cortical or subcortical landmarks that can be reproducibly identified by observers in all cases. This is applicable to a brain structure that can be clearly delineated by anatomically correct landmarks (e.g. the alveus to separate the hippocampus from the amygdala) or when other landmarks are required when an anatomical boundary cannot be consistently and reliably sampled in it's entirety (e.g. excluding much of the hippocampal tail when an extrahippocampal landmark is used as a posterior border). Between-study comparisons of hippocampal volume can only be reliably achieved when a standard MRI-based definition exists.

Manual measurements prevail for the quantification of hippocampal volume. The vast majority are simple tracing techniques, based on the methods and anatomical boundaries described by Jack *et al.* (1989), Watson *et al.* (1992) and Cook *et al.* (1992) (as reviewed by Geuze *et al.,* 2005). For these methods, the outline of the hippocampal region of interest is traced using a mouse driven cursor throughout a defined number of sections through the hippocampus, typically between 10 and 20 sections (Fig. 6). The transect

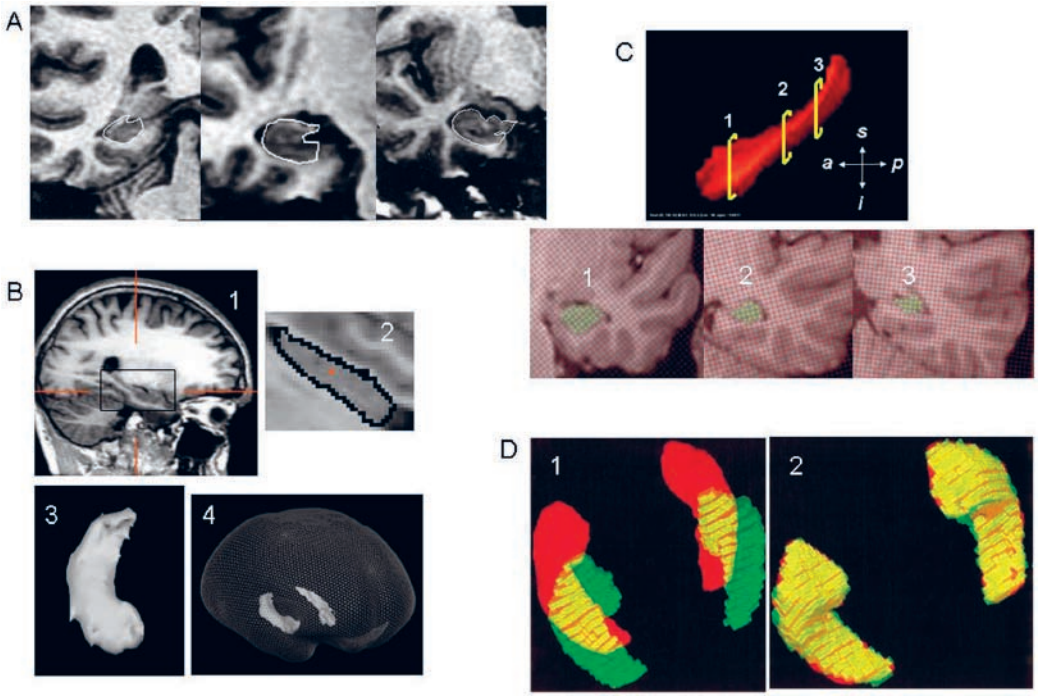

Fig. 6 - Hippocampal MRI morphometric methods. A. Manual tracing. B. Manual extraction of the hippocampus using Brainvoyager software (1. Original MR image. 2. Editing extrahippocampal tissue from the MR image. 3. 3D rendering of the extracted hippocampus. 4. Projection of the rendered hippocampi onto a glass brain). C. Stereology in conjunction with point counting (a, anterior; i, inferior; p, posterior; s, superior). Yellow points are sampled for volume estimation of the hippocampus. D. An example of automated segmentation of the hippocampi as described by Shen et al. (2002). Red = model estimation of the position of the hippocampi in a given image, Green = manual segmentation of the same hippocampi, Yellow = correspondence between methods. The figure shows before (1) and after (2) application of the deformable shape model. Excellent correspondence between methods is achieved after application of the model (2).
The colour version of this figure is available at the JASs website.

areas, determined by pixel counting within the traced region, are summed and multiplied by the distance between the consecutive sections traced to estimate hippocampal volume. Another 'drawing' method includes manually demarcating and extracting the hippocampus from the remainder of the brain, which enables a simple volume estimate (by virtue of the number of pixels within the extracted region) and an aesthetic 3D surface rendering of the hippocampus (Fig. 6). However, this latter technique is extremely labour intensive and time consuming, and may take up to two hours to demarcate a single hippocampus.

Stereology in conjunction with point counting has also been used to estimate the volume of the hippocampus from MR images (Keller *et al.,* 2002a, 2002b; Mackay *et al.,* 1998; Salmenpera *et al.,* 2005). Similar to tracing methods, hippocampal areas are determined on each equally spaced MR section, but unlike tracing methods, this is determined using stereology by counting the number of points that intersect the hippocampal transect area, which is substantially more time efficient than tracing methods. Like stereological measurement of the cerebral hemispheres, the stereological parameters for measurement of

the hippocampus are optimised to achieve a coefficient of error of less than 5% to ensure a reliable volume estimate. The stereological parameters for hippocampal volume estimates determined and applied in studies were a grid size of three and section interval of three, and like measurements of the cerebral hemispheres, resulted in approximately 200 points being counted per hippocampus (Keller *et al.,* 2002a, 2002b; Mackay *et al.,* 1998; Salmenpera *et al.,* 2005). Further to obtaining a single volume estimate of the entire hippocampus, stereological analysis also permits assessment of regional hippocampal profiles by virtue of individual section areas along the long axis of the hippocamus. Analysis of regional hippocampal profiles has revealed larger section areas in anterior regions and smaller areas in posterior regions (Keller *et al.,* 2002a), and regional hippocampal atrophy due to disease (Keller *et al.,* 2002a; Woermann *et al.,* 1998). An example of stereological measurement of the hippocampus is provided in Figure 6.

Automatic extraction of the hippocampus on MR images is difficult (Parker & Chard, 2003). However, there are several semi-automated hippocampal morphometric techniques that employ different methods to extract hippocampal volume. Cardenas *et al.* (2003) employed pattern matching techniques to map a hippocampal template to each participant's hippocampi and subsequently used 22 separate anatomical landmarks to guide matching of the hippocampus, which yielded a high test-retest reliability (intraclass correlation (ICC) = 0.97 for both hippocampi). Hippocampal segmentation using general pattern matching is obtained using a hippocampal template, which represents an average atlas of the hippocampus. The template is applied as a priori information for the spatial distribution of hippocampal tissue on individual MR images. Segmentation is aided by manual placing of separate anatomical landmarks along the inferior, superior, medial and lateral limits of the hippocampus at equal lengths along its axis. Semi-automated methods that warp a hippocampal template to an individual MR image in conjunction with user-defined points placed on hippocampal boundaries achieve a high degree of accuracy for hippocampal segmentation (Csernansky *et al.,* 1998; Csernansky *et al.,* 2002; Haller *et al.,* 1996, 1997). However, these methods are based on matching the signal intensity – and not the shape – of the grey matter of the target hippocampus to the template hippocampus. Restricting analysis based on signal intensity is problematic considering the similar signal intensities of adjacent grey matter structures such as the amygdala and parahippocampal gyrus. Therefore, this approach theoretically could be compromised in patients with abnormalities (e.g. atrophy, developmental malformations) of the medial temporal lobe (Shen *et al.,* 2002).

Shen *et al.* (2002) described a deformable shape model for measurements of the size and shape of the hippocampus, which includes information about the geometry of the hippocampus and a priori information of hippocampal structure (by virtue of a template based on a representative population of people). The model is placed close to the hippocampus and deforms with respect to both the geometry of the target hippocampus and the a priori information of local medial temporal lobe tissue on individual images (Fig. 6). To help the deformable model extract the hippocampus from extrahippocampal tissue, the algorithm additionally utilises several manual defined points placed on hippocampal boundaries. This method yields excellent agreement with manual segmentation by expert raters (ICC = 0.97). Other semi-automated hippocampal deformation and warping techniques have been applied to study pathological hippocampal changes and were found to be reliable when compared to manual tracing methods (Crum *et al.,* 2001; Hogan *et al.,* 2000a, 2000b, 2003, 2004). There are also tools available that determine hippocampal morphological changes over time based on an automatically rendered 3D hippocampal mesh generated from manual tracing methods on MR images obtained at different time points, which may provide important information on disease progression (Thompson *et al.,* 2004).

Broca's area

There are various macroscopic (i.e. gyral) and microscopic (i.e. cytoarchitectonic) definitions of Broca's area. Ordinarily, the sulcal contours of the inferior frontal gyrus and rami of the Sylvian fissure define this area on a gross anatomical level, and area 44 and area 45 on a cytoarchitectonic level (Amunts *et al.,* 1999, 2003; Keller *et al.,* 2007c, 2009). It is important to note that gyral and cytoarchitectonic borders defining Broca's area do not align in the human or great ape brain, and the reader is referred to Keller *et al.* (2009) and the references therein for a detailed discussion of the distinction between macroscopic and microscopic definitions of Broca's area. This manuscript is concerned with macroscopic definitions of Broca's area, given that the microscopic structure of this region is beyond the resolution of standard MRI.

In patients with various forms of aphasia and hemiparesis it was noted on autopsy that the left cerebral hemisphere was damaged due to infarction of the upper regions of the middle cerebral artery, and the most extensive damage was located in the posterior regions of the third frontal convolution – or inferior frontal gyrus (Broca, 1861a, 1861b, 1863, 1865). The work of Paul Broca and some other influential authors (for review see Finger & Roe, 1999) provided the first scientific evidence for functional localisation in the human brain. The work of Broca ascribed importance of middle and posterior regions of the left inferior frontal gyrus to the expression of speech. However, circumscribed damage to the inferior frontal gyrus in patients with infarction of the middle cerebral artery is unlikely, given the likelihood of diffuse damage in other frontal, temporal, parietal and subcortical regions (Mohr, 1979). This has complicated the definition of Broca's area given that damage to many cortical and subcortical regions can generate the kind of aphasia that Broca reported. Furthermore, Broca's area exhibits great inter-individual variability in structure (Keller *et al.,* 2007c, 2009), which makes a standardised definition for quantitative assessment difficult.

The vast majority of human studies defining the gross morphology of Broca's area use the sulcal contours of middle and posterior regions of the inferior frontal gyrus as delineating landmarks (see Keller *et al.* (2009) for a detailed review). The inferior frontal gyrus can be divided into three subregions – a posterior third (pars opercularis), a middle third (pars triangularis) and an anterior third (pars orbitalis). MRI definitions of Broca's area typically exclude the pars orbitalis and delineate the pars opercularis and pars triangularis using the contours of the inferior frontal sulcus, inferior precentral sulcus, and anterior rami of the Sylvian fissure (see Keller *et al.* (2007c, 2009) for detailed anatomical descriptions). Whilst the lateral-medial and anterior-posterior extent of the inferior frontal gyrus may differ between studies, the vast majority quantify some aspect of the pars opercularis and / or pars triangularis for a volume estimate of Broca's area.

Although Broca's area was defined based on human language, an homologous region has been argued to exist in the great ape brain (Cantalupo & Hopkins, 2001; Sherwood *et al.,* 2003). This region of cortex may share some functional similarities in both humans and non-human primates, such as orofacial musculature (Petrides *et al.,* 2005), the mirror neurons phenomenon (Nelissen *et al.,* 2005) and communicative signalling (Taglialatela *et al.,* 2008). However, there are some significant differences in structure of this region between humans and great apes. For example, whilst the anterior rami of the Sylvian fissure delineate the pars opercularis and pars triangularis in humans, these rami are not present in the great apes, and the fronto-orbital sulcus, which is not present in humans, delineates the anterior portion of the pars opercularis in the chimpanzee, bonobo, and gorilla brain (Cantalupo & Hopkins, 2001; Sherwood *et al.,* 2003). Therefore quantitative MR image analysis methods must be adapted to consider inter-species differences in comparative anatomy.

There are various quantitative MRI techniques that have been used to prospectively assess

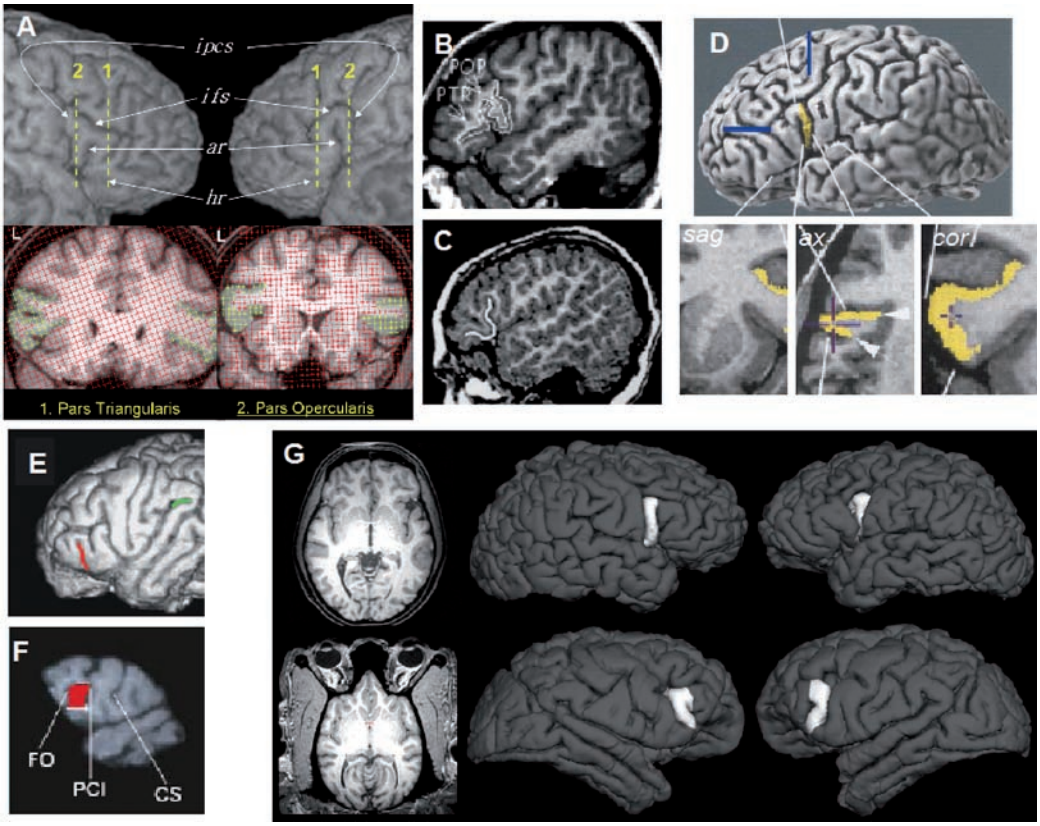

Fig. 7 - MRI Methods used to estimate the size of Broca's area in humans and non-human primates. A. Stereology in conjunction with point counting for volume estimation in humans (from Keller et al. (2007c)). Yellow points are sampled within the pars triangularis and pars opercularis. The approximate location of the coronal sections (bottom) are indicated on the 3D lateral brain renderings (top) (ar, ascending ramus of the Sylvian fissure; hr, horizontal ramus of the Sylvian fissure; ifs, inferior frontal sulcus; ipcs, inferior precentral sulcus). B. Tracing method described by Knaus et al. (2006) for volume estimation of the pars opercularis (POP) and pars triangularis (PTR) in humans. C. Tracing method on sagittal sections described by Eckert et al. (2003) to determine the length of the anterior rami of the Sylvian fissure for estimation of the size of the pars triangularis in humans. D. Painting of the grey matter within the pars opercularis using orthogonal sections and a 3D lateral brain rendering as described by Tomaiuolo et al. (1999) (ax, axial view; cor, coronal view; sag, sagittal view). E. Similar to the method described by Eckert et al. (2003) in (C), the length of the fronto-orbital sulcus (red line) is determined in the great ape brain to estimate the size of Broca's area homologue (Hopkins et al., 2007). F. Tracing method on sagittal sections used to obtain a surface area of the pars opercularis in the great ape brain described by Cantalupo and Hopkins (2001) (CS, central sulcus; FO, fronto-orbital sulcus; PCI, inferior precentral sulcus). G. To date there has not been a direct comparison of the morphology of Broca's area in humans and Broca's area homologue in the great ape brain using identical MRI methods. This is an illustration of volume estimation of the pars opercularis in a human (top) and a chimpanzee (bottom) brain from high resolution MR images acquired using the same MRI scanner, almost identical image acquisition parameters and identical MR image analysis techniques and software (FREESURFER). True comparative quantitative analyses such as these may be able to directly elucidate whether cerebral asymmetries are human-specific or shared by our evolutionary ancestors.
The colour version of this figure is available at the JASs website.

the morphology of Broca's area in humans and non-human primates (Cantalupo & Hopkins, 2001; Eckert *et al.,* 2003; Foundas *et al.,* 1995, 1996, 1998, 2001; Hopkins *et al.,* 2007; Keller *et al.,* 2007c; Knaus *et al.,* 2006, 2007; Tomaiuolo *et al.,* 1999). Tracing methods have been applied by using a mouse driven cursor to draw around the convolutions of interest (i.e. the pars triangularis or pars opercularis) primarily on sagittal sections (Fig. 7), although the number of sagittal sections used for analysis has varied between studies. The number of sagittal sections traced have been defined based on a stereotaxic coordinate system after spatial normalisation (Foundas *et al.,* 1996, 1998, 2001), at the structure's greatest extent (Foundas *et al.,* 1995), or until the insula appears (Cantalupo & Hopkins, 2001). Sagittal sections allow optimum visualisation of the anterior-posterior extent of the inferior frontal gyrus and the dorsal border, that is, the inferior frontal sulcus. It is however difficult to sample the entire gyrus to its medial-most extent (i.e. to the fundus of sulci) using only sagittal sections, given the ambiguity associated with the separation of the inferior frontal gyrus from the insula and other regions from this orientation. It is therefore not surprising that all of the aforementioned sagittal tracing studies did not obtain a volume estimate of the entire gyrus.

Coronal sections enable optimal visualisation of the depth of the inferior frontal gyrus. We have previously measured the grey matter within the pars opercularis and pars triangularis on coronal sections using stereology in conjunction with point counting using the fundus of sulci to guide measurements (Keller *et al.,* 2007c, Fig. 7). We reported that the optimal stereological parameters for the pars opercularis and pars triangularis were a grid size of three (similarly to the hippocampus), and every section for the pars opercularis and every second section for the pars triangularis, given the ordinarily larger length of the latter (Keller *et al.,* 2007c). Again, at least 200 points were sampled, and a coefficient of error under 5% obtained. Given that sagittal sections permit optimal visualisation of the anterior-posterior extent of the inferior frontal gyrus, it is necessary to place markers in appropriate boundaries to guide measurements in the coronal plane (for example, to delineate the section at the front (e.g. using the anterior horizontal ramus of the Sylvian fissure) and back (e.g. using the inferior precentral sulcus) of the region of interest that informs the investigator to start and stop measurements).

The vast majority of methods measure brain structures using one orientation. However, many structures – including Broca's area – have complex 3D anatomy, and the development of software packages to measure brain structures using all three orthogonal sections is important. Both MEASURE and DISPLAY software packages (Appendix) permit simultaneous visualisation of axial, sagittal and coronal sections during measurements. In particular, DISPLAY has been used to estimate the volume of the pars opercularis by labelling grey matter voxels using a painting technique (Tomaiuolo *et al.,* 1999), which allowed visualisation of all labelled voxels in all three orthogonal planes in conjunction with a lateral rendering of the cerebral hemisphere. Volume estimation of Broca's area using orthogonal sections is also possible using stereology in conjunction with point counting using MEASURE software. Wherever possible, brain structures with complex morphology should be measured using multiple orthogonal views to ensure anatomical specificity of the sampled region. Finally, it is also possible to obtain volume, surface area and cortical thickness measurements from the surface of the brain, by labelling the sulcal contours that define the region of interest using FREESURFER software. For this method, once the cortical surface is reconstructed (which can process one to five brains per day, depending on the processing power of the computer), creating the label defining Broca's area is extremely time efficient, taking up to ten minutes per brain (pars opercularis and pars triangularis bilaterally). We are currently applying these methods in conjunction with stereology to obtain volume estimates of Broca's area in humans and Broca's area homologue in non-human primates (Fig. 7).

Conclusion

There are many choices available to a research group for quantitative MRI of the brain. Discussion in the current article was exclusive to volume estimation, and pertained to the software and techniques familiar to the authors. We have provided sufficient information for volume estimation of three brain structures that are of particular interest in cognitive, clinical and comparative neuroscience. The prerequisites for quantitative MRI of the brain include repeatable and reproducible volume estimates obtained from reliable methods, and well-defined anatomical guidelines for quantification.

Acknowledgements

This work was supported by a European Commission Grant from the Sixth Framework Programme entitled 'Paul Broca II – The Evolution of Cerebral Asymmetry in Homo Sapiens' Project no. 12880. We also thank two anonymous reviewers and Marta Garcia-Finana at the University of Liverpool for their helpful remarks on an earlier version of this manuscript.

Info on the web

http://w1.siemens.com/entry/cc/en/#healthcare.xml-452770-0-0
Information of Siemens MR systems

http://www.quantificare.com/
Dedicated to Medical Image Processing applications

http://health.howstuffworks.com/mri.htm
A simple overview of the basic principles of MRI

http://www.stereologysociety.org/
International Society for Stereology

http://www.fil.ion.ucl.ac.uk/spm/
SPM for structural and functional analysis of MR images

http://www.fmrib.ox.ac.uk/fsl/
FSL for structural and functional analysis of MR images

http://www.brainvoyager.com/
Brainvoyager for structural and functional analysis of MR images

http://surfer.nmr.mgh.harvard.edu/
Freesurfer for structural and functional analysis of MR images

References

Amunts K., Schleicher A., Burgel U., Mohlberg H., Uylings H. & Zilles K. 1999. Broca's region revisited: cytoarchitecture and intersubject variability. *J. Comp. Neurol.*, 412: 319-341.

Amunts K., Schleicher A., Ditterich A. & Zilles K. 2003. Broca's region: cytoarchitectonic asymmetry and developmental changes. *J. Comp. Neurol.*, 465: 72-89.

Andreasen N.C., Rajarethinam R., Cizadlo T., Arndt S., Swayze V.W., Flashman L.A, *et al.* 1996. Automatic atlas-based volume estimation of human brain regions from MR images. *J. Comput. Assist. Tomogr.*, 20: 98-106.

Ashburner J. & Friston K.J. 2000. Voxel-based morphometry – the methods. *Neuroimage*, 11: 223-232.

Ashburner J. & Friston K.J. 2001. Why voxel-based morphometry should be used. *Neuroimage*, 14: 1238-1243.

Ashtari M., Barr W.B., Schaul N. & Bogerts B. 1991. Three-dimensional fast low-angle shot imaging and computerized volume measurement of the hippocampus in patients with chronic epilepsy of the temporal lobe. *AJNR Am. J. Neuroradiol.*, 12: 941-947.

Barrick T.R., Mackay C.E., Prima S., Maes F., Vandermeulen D., Crow T.J. & Roberts., N. 2005. Automatic analysis of cerebral asymmetry: an exploratory study of the relationship between brain torque and planum temporale asymmetry. *Neuroimage*, 24: 6786-91.

Barta P.E., Dhingra L., Royall R. & Schwartz E. 1997. Improving stereological estimates for the volume of structures identified in three-dimensional arrays of spatial data. *J. Neurosci. Methods*, 75: 111-118.

Becker T., Elmer K., Schneider F., Schneider M., Grodd W., Bartels M., *et al.* 1996. Confirmation of reduced temporal limbic structure volume on magnetic resonance imaging in male patients with schizophrenia. *Psychiatry Res.*, 67: 135-143.

Bookstein F.L. 2001. "Voxel-based morphometry" should not be used with imperfectly registered images. *Neuroimage*, 14: 1454-1462.

Brambilla P., Harenski K., Nicoletti M., Sassi R.B., Mallinger A.G., Frank E., *et al.* 2003. MRI investigation of temporal lobe structures in bipolar patients. *J. Psychiatr. Res.*, 37: 287-295.

Bremner J.D., Randall P., Scott T.M., Bronen R.A. Seibyl J.P., Southwick S.M., *et al.* 1995. MRI-based measurement of hippocampal volume in patients with combat-related posttraumatic stress disorder. *Am. J. Psychiatry*, 152: 973-981.

Broca P. 1861a. Nouvelle observation aphémie produite par un lésion de la moité postérieure des deuxième et troisième circonvolutions frontales. *Bulletins de la Société Anatomique de Paris*, 6: 398-407.

Broca P. 1861b. Remarques sur le Siége de la Faculté du Langage Articulé, Suivies d'une Observatoin d'aphémie (Perte de la Parole). *Bulletin de la Société Anatomique de Paris*, 6: 330-357.

Broca P. 1863. Localisation des fonctions cérébrales. Siège du langage articulé. *Bulletins de la Société d'Anthropologie*, 4: 200-204.

Broca P. 1865. Sur le siège de la faculté du langage articule. *Bulletins de la Société d'Anthropologie*, 6: 377-393.

Cantalupo C. & Hopkins WD. 2001. Asymmetric Broca's area in great apes. *Nature*, 414: 505.

Caramanos Z., Venugopal R., Collins D.L., MacDonald D., Evans A.C. & Petrides M. 1997. Human brain sulcal anatomy: an MRI-based study. *Hum. Brain. Mapp.*, 4: 350.

Cardenas V.A., Du A.T., Hardin D., Ezekiel F., Weber P., Jagust W.J., *et al.* 2003. Comparison of methods for measuring longitudinal brain change in cognitive impairment and dementia. *Neurobiol. Aging*, 24: 537-544.

Collins D.L., Holmes T.M., Peters T.M. & Evans A.C. 1995. Automatic 3D model-based neuroanatomical segmentation. *Hum. Brain. Mapp.*, 3: 190-208.

Collins D.L. & Neelin P., Peters T.M., Evans A.C. 1994. Automatic 3D intersubject registration of MR volumetric data in standardized Talairach space. *J. Comput. Assist. Tomogr.*,18: 192-205.

Cook M.J., Fish D.R., Shorvon S.D., Straughan K. & Stevens J.M. 1992. Hippocampal volumetric and morphometric studies in frontal and temporal lobe epilepsy. *Brain*, 115: 1001-1015.

Cowell P.E., Sluming V.A., Wilkinson I.D., Cezayirli E., Romanowski C.A., Webb J.A., Keller S.S., Mayes A. & Roberts N. 2007. Effects of sex and age on regional prefrontal brain volume in two human cohorts. *Eur. J. Neurosci.* 25: 307-318.

Crum W.R., Scahill R.I. & Fox N.C. 2001. Automated hippocampal segmentation by regional fluid registration of serial MRI: validation and application in Alzheimer's disease. *Neuroimage*, 13: 847-855.

Csernansky J.G., Joshi S., Wang L., Haller J.W., Gado M., Miller J.P., *et al.* 1998. Hippocampal morphometry in schizophrenia by high dimensional brain mapping. *Proc. Natl. Acad. Sci. USA*, 95: 11406-11411.

Csernansky J.G., Wang L., Jones D., Rastogi-Cruz D., Posener J.A., Heydebrand G. *et al.* 2002. Hippocampal deformities in schizophrenia characterized by high dimensional brain mapping. *Am. J. Psychiatry*, 159: 2000-2006.

Deichmann R., Schwarzbauer C. & Turner R. 2004. Optimisation of the 3D MDEFT sequence for anatomical brain imaging: technical implications at 1.5 and 3 T. *Neuroimage*, 21: 757-767.

Doherty C.P., Fitzsimons M., Holohan T., Mohamed H.B., Farrell M., Meredith G.E. & Staunton H. 2000. Accuracy and validity of stereology as a quantitative method for assessment of human temporal lobe volumes acquired my magnetic resonance imaging. *Magn. Reson. Imaging*, 18: 1017-1025.

Duvernoy HM. 1998. *The human hippocampus*. New York: Springer-Verlag.

Eckert M.A., Leonard C.M., Richards T.L., Aylward E.H., Thomson J. & Berninger V.W. 2003. Anatomical correlates of dyslexia: frontal and cerebellar findings. *Brain*, 126: 482-494.

Filipek P.A., Richelme C., Kennedy D.N. & Caviness V.S., Jr. 1994. The young adult human brain: an MRI-based morphometric analysis. *Cereb. Cortex*, 4: 344-360.

Finger S. & Roe D. 1999. Does Gustave Dax deserve to be forgotten? The temporal lobe theory and other contributions of an overlooked figure in the history of language and cerebral dominance. *Brain Lang.*, 69: 16-30.

Foundas A.L., Eure K.F., Luevano L.F. & Weinberger D.R. 1998. MRI asymmetries of Broca's area: the pars triangularis and pars opercularis. *Brain Lang.*, 64: 282-296.

Foundas A.L, Leonard C.M, Gilmore R.L, Fennell E.B. & Heilman K.M. 1996. Pars triangularis asymmetry and language dominance. *Proc. Natl. Acad. Sci. USA*, 93: 719-722.

Foundas A.L, Leonard C.M. & Heilman K.M. 1995. Morphologic cerebral asymmetries and handedness. The pars triangularis and planum temporale. *Arch. Neurol.*, 52: 501-508.

Foundas A.L., Weisberg A., Browning C.A. & Weinberger D.R. 2001. Morphology of the frontal operculum: a volumetric magnetic resonance imaging study of the pars triangularis. *J. Neuroimaging*, 11: 153-159.

Freeborough P.A, Fox N.C. & Kitney R.I. 1997. Interactive algorithms for the segmentation and quantitation of 3-D MRI brain scans. Comput. *Methods Programs Biomed.*, 53: 15-25.

García-Fiñana M., Cruz-Orive L., Mackay C., Pakkenberg B. & Roberts N. 2003. Comparison of MR imaging against physical sectioning to estimate the volume of human cerebral compartments. *Neuroimage*, 18: 505-516.

García-Fiñana M. & Cruz-Orive L. 2000. New approximations for the variance in Cavalieri sampling. *J. Microsc.*, 199: 224-238.

García-Fiñana M., Keller S.S. & Roberts N. 2009. Confidence intervals for the volume of brain structures in Cavalieri sampling with local errors. *J. Neurosci. Methods*, 179: 71-77.

Geuze E., Vermetten E. & Bremner J.D. 2005. MR-based in vivo hippocampal volumetrics: 1. Review of methodologies currently employed. *Mol. Psychiatry*, 10: 147-159.

Gong Q.Y., Tan L.T., Romaniuk C.S., Jones B., Brunt J.N. & Roberts N. 1999. Determination of tumour regression rates during radiotherapy for cervical carcinoma by serial MRI: comparison of two measurement techniques and examination of intraobserver and interobserver variability. *Br. J. Radiol.*, 72: 62-72.

Good C.D., Scahill R.I., Fox N.C., Ashburner J., Friston K.J., Chan D. *et al.* 2002. Automatic differentiation of anatomical patterns in the human brain: validation with studies of degenerative dementias. *Neuroimage*, 17: 29-46.

Hackert V.H., den Heijer T., Oudkerk M., Koudstaal P.J., Hofman A. & Breteler M.M.

2002. Hippocampal head size associated with verbal memory performance in nondemented elderly. *Neuroimage*, 17: 1365-1372.

Haller J.W., Banerjee A., Christensen G.E., Gado M., Joshi S., Miller M.I., *et al.* 2002. Three-dimensional hippocampal MR morphometry with high-dimensional transformation of a neuroanatomic atlas. *Radiology*, 202: 504-510.

Haller J.W., Christensen G.E., Joshi S.C., Newcomer J.W., Miller M.I., Csernansky J.G., *et al.* 1996. Hippocampal MR imaging morphometry by means of general pattern matching. *Radiology*, 199: 787-791.

Hogan R.E., Bucholz R.D. & Joshi S. 2003. Hippocampal deformation-based shape analysis in epilepsy and unilateral mesial temporal sclerosis. *Epilepsia*, 44: 800-806.

Hogan R.E., Mark K.E., Choudhuri I., Wang L., Joshi S., Miller M.I., *et al.* 2000a. Magnetic resonance imaging deformation-based segmentation of the hippocampus in patients with mesial temporal sclerosis and temporal lobe epilepsy. *J. Digit. Imaging*, 13: 217-218.

Hogan R.E., Mark K.E., Wang L., Joshi S., Miller M.I. & Bucholz R.D. 2000b. Mesial temporal sclerosis and temporal lobe epilepsy: MR imaging deformation-based segmentation of the hippocampus in five patients. *Radiology*, 216: 291-297.

Hogan R.E., Wang L., Bertrand M.E., Willmore L.J., Bucholz R.D., Nassif A.S., *et al.* 2004. MRI-based high-dimensional hippocampal mapping in mesial temporal lobe epilepsy. *Brain*, 127: 1731-1740.

Hopkins W.D., Russell J.L. & Cantalupo C. 2007. Neuroanatomical correlates of handedness for tool use in chimpanzees (Pan troglodytes): implication for theories on the evolution of language. *Psychol. Sci.*, 18: 971-977.

Jack C.R., Jr., Twomey C.K., Zinsmeister A.R., Sharbrough F.W., Petersen R.C. & Cascino G.D. 1989. Anterior temporal lobes and hippocampal formations: normative volumetric measurements from MR images in young adults. *Radiology*, 172: 549-554.

Jacobsen L.K., Giedd J.N., Vaituzis A.C., Hamburger S.D., Rajapakse J.C., Frazier J.A., *et al.* 1996. Temporal lobe morphology in childhood-onset schizophrenia. *Am. J. Psychiatry*, 153: 355-361.

Keller S.S., Cresswell P., Denby C., Wieshmann U., Eldridge P., Baker G. & Roberts, N. 2007a. Persistent seizures following left temporal lobe surgery are associated with posterior and bilateral structural and functional brain abnormalities. *Epilepsy Res.*, 74: 131-139.

Keller S.S., Crow T., Foundas A., Amunts K. & Roberts N. 2009. Broca's area: nomenclature, anatomy, typology and asymmetry. *Brain Lang.*, 109: 29-48.

Keller S.S., Deppe M., Roberts N., Garcia-Finana M., Ringelstein E. & Knecht S. 2007b. *Cortical asymmetry and language lateralisation: insula and not classical language cortex predicts cerebral dominance*. Organisation of Human Brain Mapping. Chicago, USA.

Keller S.S., Highley J.R., Garcia-Finana M., Sluming V., Rezaie R. & Roberts N. 2007c. Sulcal variability, stereological measurement and asymmetry of Broca's area on MR images. *J. Anat.*, 211: 534-555.

Keller S.S., Mackay C.E., Barrick T.R., Wieshmann U.C., Howard M.A. & Roberts N. 2002a. Voxel-based morphometric comparison of hippocampal and extrahippocampal abnormalities in patients with left and right hippocampal atrophy. *Neuroimage*, 16: 23-31.

Keller S.S. & Roberts N. 2008. Voxel-based morphometry of temporal lobe epilepsy: An introduction and review of the literature. *Epilepsia*, 49: 741-757.

Keller S.S., Wieshmann U.C., Mackay C.E., Denby C.E., Webb J. & Roberts N. 2002b. Voxel based morphometry of grey matter abnormalities in patients with medically intractable temporal lobe epilepsy: effects of side of seizure onset and epilepsy duration. *J. Neurol. Neurosurg. Psychiatry*, 73: 648-655.

Keller S.S., Wilke M., Wieshmann U.C., Sluming V.A. & Roberts N. 2004. Comparison of standard and optimized voxel-based morphometry for analysis of brain changes associated with temporal lobe epilepsy. *Neuroimage*, 23: 860-868.

Knaus T.A., Bollich A.M., Corey D.M., Lemen L.C. & Foundas A.L. 2006. Variability in perisylvian brain anatomy in healthy adults. *Brain Lang.*, 97: 219-232.

Knaus T.A., Corey D.M., Bollich A.M., Lemen L.C. & Foundas A.L. 2007. Anatomical asymmetries of anterior perisylvian speech-language regions. *Cortex*, 43: 499-510.

Lencz T., McCarthy G., Bronen R.A., Scott T.M., Inserni J.A., Sass K.J., *et al.* 1992. Quantitative magnetic resonance imaging in temporal lobe epilepsy: relationship to neuropathology and neuropsychological function. *Ann. Neurol.*, 31: 629-637.

Lim K.O., Zipursky R.B., Murphy G.M., Jr. & Pfefferbaum A. 1990. In vivo quantification of the limbic system using MRI: effects of normal aging. *Psychiatry Res.*, 35: 15-26.

MacDonald D. 1998. *A method for identifying geometrically simple surfaces from three dimensional images*. PhD Thesis. McGill University. Montreal.

Mackay C.E., Roberts N., Mayes A.R., Downes J.J., Foster J.K. & Mann D. 1998. An exploratory study of the relationship between face recognition memory and the volume of medial temporal lobe structures in healthy young males. *Behav. Neurol.*, 11: 3-20.

Maes F., Van Leemput K., DeLisi L., Vandermeulen D. & Suetens P. 1999. Quantification of cerebral grey and white matter asymmetry from MRI, lecture notes in computer science. In Taylor C. & Colchester A. (eds): *Proceedings 2nd International Conference on Medical Image Computing and Computer-Assisted Intervention, MICCAI'99*, pp. 348– 357. Springer, Cambridge,.

Marsh L., Morrell M.J., Shear P.K., Sullivan E.V., Freeman H., Marie A., *et al.* 1997. Cortical and hippocampal volume deficits in temporal lobe epilepsy. *Epilepsia*, 38: 576-587.

Mohr J.P. 1979. Broca's area and Broca's aphasia. In Whitaker H. & Whitaker H.A. (eds): *Studies in neurolinguistics*. Elsevier, New York.

Nelissen K., Luppino G., Vanduffel W., Rizzolatti G. & Orban G. A. 2005. Observing others: Multiple action representation in the frontal lobe. *Science*, 310: 332–336.

Pantel J., O'Leary D.S., Cretsinger K., Bockholt H.J., Keefe H., Magnotta V.A., *et al.* 2000. A new method for the in vivo volumetric measurement of the human hippocampus with high neuroanatomical accuracy. *Hippocampus*, 10: 752-758.

Parker G. & Chard D. 2003. Volume and Atrophy. In P. Tofts (ed): *Quantitative MRI of the brain: measuring changes caused by disease*. John Wiley and Sons, New York.

Petrides M., Cadoret G. & Mackey S. 2005. Orofacial somatomotor responses in the macaque monkey homologue of Broca's area. *Nature*, 435: 1235–1238.

Pruessner J.C., Li LM, Serles W., Pruessner M., Collins D.L., Kabani N., *et al.* 2000. Volumetry of hippocampus and amygdala with high-resolution MRI and three-dimensional analysis software: minimizing the discrepancies between laboratories. *Cereb. Cortex*, 10: 433-442.

Reiss A.L., Lee J. & Freund L. 1994. Neuroanatomy of fragile X syndrome: the temporal lobe. *Neurology*, 44: 1317-24.

Roberts N., Puddephat M.J. & McNulty V. 2000. The benefit of stereology for quantitative radiology. *Br. J. Radiol.*, 73: 679-697.

Roberts N., Howard C., Cruz-Orive L. & Edwards R. 1991. The application of total vertical projections for the unbiased estimation of the length of blood vessels and other structures by magnetic resonance imaging. *Magn. Reson. Imaging*, 9:917-925.

Ronan L., Doherty C.P., Delanty N., Thornton J., & Fitzsimons M. 2006. Quantitative MRI: a reliable protocol for measurement of cerebral gyrification using stereology. *Magn. Reson. Imaging*, 24: 265-272.

Ronan L., Murphy K., Delanty N, Doherty C., Maguire S., Scanlon C. & Fitzsimons M. 2007. Cerebral cortical gyrification: a preliminary investigation in temporal lobe epilepsy. *Epilepsia*, 48: 211-219.

Rorden C. & Brett M. 2000. Stereotaxic display of brain lesions. *Behav. Neurol.*, 12: 191-200.

Salmenpera T., Kononen M., Roberts N., Vanninen R., Pitkanen A. & Kalviainen R. 2005.

Hippocampal damage in newly diagnosed focal epilepsy: a prospective MRI study. *Neurology*, 64: 62-68.

Sheline Y.I., Black K.J., Lin D.Y., Christensen G.E., Gado M.H. Brunsden B.S. & Vannier M.W. 1996. Stereological MRI volumetry of the frontal lobe. *Psychiatry Res*., 67: 203-214.

Shen D., Moffat S., Resnick S.M. & Davatzikos C. 2002. Measuring size and shape of the hippocampus in MR images using a deformable shape model. *Neuroimage*, 15: 422-434.

Shenton M.E., Kikinis R., Jolesz F.A., Pollak S.D., LeMay M., Wible C.G., *et al.* 1992. Abnormalities of the left temporal lobe and thought disorder in schizophrenia. A quantitative magnetic resonance imaging study. *N. Engl. J. Med*., 327: 604-612.

Sherwood C.C., Broadfield D.C., Holloway R.L., Gannon P.J. & Hof P.R. 2003. Variability of Broca's area homologue in African great apes: implications for language evolution. Anat. Rec. A Discov. *Mol. Cell. Evol. Biol*., 271: 276-285.

Sisodiya S., Free S., Fish D. & Shorvon S. 1996. MRI-based surface area estimates in the normal adult human brain: evidence for structural organisation. *J. Anat*., 188: 425-438.

Spencer S.S., McCarthy G. & Spencer D.D. 1993. Diagnosis of medial temporal lobe seizure onset: relative specificity and sensitivity of quantitative MRI. *Neurology*, 43: 2117-2124.

Taglialatela J., Russell J., Schaeffer J. & Hopkins W. 2008. Communicative signalling activates ‚Broca's' homologue in chimpanzees. *Curr. Biol*., 18: 343-348.

Theodore W.H., Bhatia S., Hatta J., Fazilat S., DeCarli C., Bookheimer S.Y., *et al.* 1999. Hippocampal atrophy, epilepsy duration, and febrile seizures in patients with partial seizures. *Neurology*, 52: 132-136.

Theodore W.H. & Gaillard W.D. 1999. Association between hippocampal volume and epilepsy duration. *Ann. Neurol*.,46: 800.

Theodore W.H., Gaillard W.D., De Carli C., Bhatia S. & Hatta J. 2001. Hippocampal volume and glucose metabolism in temporal lobe epileptic foci. *Epilepsia*, 42: 130-132.

Thompson P.M., Hayashi K.M., De Zubicaray G .I., Janke A.L., Rose S.E., Semple J., *et al.* 2004. Mapping hippocampal and ventricular change in Alzheimer disease. *Neuroimage*, 22: 1754-1766.

Toga A.W. & Mazziotta J. 2002. *Brain mapping: the methods*. Elsevier.

Tomaiuolo F, MacDonald J.D., Caramanos Z., Posner G., Chiavaras M., Evans A.C., *et al.* 1999. Morphology, morphometry and probability mapping of the pars opercularis of the inferior frontal gyrus: an in vivo MRI analysis. *Eur. J. Neurosci*., 11: 3033-3046.

Watson C., Andermann F., Gloor P., Jones-Gotman M., Peters T., Evans A., *et al.* 1992. Anatomic basis of amygdaloid and hippocampal volume measurement by magnetic resonance imaging. *Neurology*, 42: 1743-1750.

Wilke M., Kassubek J., Ziyeh S., Schulze-Bonhage A. & Huppertz H.J. 2003. Automated detection of gray matter malformations using optimized voxel-based morphometry: a systematic approach. *Neuroimage*, 20: 330-343.

Woermann F.G., Barker G.J., Birnie K.D., Meencke H.J. & Duncan J.S. 1998. Regional changes in hippocampal T2 relaxation and volume: a quantitative magnetic resonance imaging study of hippocampal sclerosis. *J. Neurol. Neurosurg. Psychiatry*, 65: 656-664.

Zipursky R.B., Marsh L., Lim K.O., DeMent S., Shear P.K., Sullivan E.V., *et al.* 1994. Volumetric MRI assessment of temporal lobe structures in schizophrenia. *Biol. Psychiatry*, 35: 501-516.

Associate Editor, Emiliano Bruner

Appendix 1 - Some software packages available for MR image transformations and volume estimation.

Software	Reference	Software and Hardware Compatibility	Cost	Functions	User Expertise
AFNI	Medical College of Wisconsin, Milkwaukee, US; http://afni.nimh.nih.gov/afni/	Runs on Linux, Mac OS, and SUN	Free	2D and 3D image viewing, reformatting	Knowledge of image orientation and gross neuroanatomy
ANALYZE	MAYO Foundation, Minnesota, US; http://ndc.mayo.edu/mayo/research/robb_lab/analyze.cfm	Runs on Windows, Linux or SUN	Price depends on license type	2D and 3D image viewing, reformatting, ROI demarcation and extraction, ROI quantification using stereology or tracing, cortical reconstruction	Knowledge of image orientation, quantification and gross neuroanatomy, depending on investigator's needs
ANIMAL	Montreal Neurological Institute, McGill University, Canada; Collins et al. (1994, 1995); www.bic.mni.mcgill.ca/users/louis/MNI_ANIMAL_home/readme	Runs on Linux and SUN	Free	Spatial normalization of MR images	Procedure is performed automatically by the computer
BrainVoyager	Brain Innovation; www.brainvoyager.com	Runs on Windows, Linux or Mac OS	Price depends on license type	2D and 3D image viewing, reformatting, ROI demarcation and extraction, basic ROI quantification, tissue segmentation and cortical reconstruction	Depends on investigator needs. Segmentation is automated, but ROI demarcation and extraction requires investigator expertise in neuroanatomy
Brains	University of Iowa Hospitals and Clinics, College of Medicine, Iowa City, IA, US; Andreasen et al. (1996); www.nitrc.org/projects/brains	Runs on Mac OS	Free	2D and 3D image viewing, ROI quantification, tissue segmentation, surface reconstruction	Neuroanatomical knowledge for ROI quantification, other computer automated processes available
Caret	Van Essen Laboratory, Washington University in St. Louis, US; http://brainmap.wustl.edu/caret	Runs on Windows, Linux and Mac OS	Free	2D and 3D image viewing, reformatting, brain extraction, tissue segmentation, cortical reconstruction, cortical inflation, flatmapping, probabilistic mapping	Depends on investigator needs. Many interactive (manual) and computer intensive (automated) operations

***Appendix 1* (continued)**

Software	Reference	Software and Hardware Compatibility	Cost	Functions	User Expertise
Display	Montreal Neurological Institute, McGill University, Canada; MacDonald (1998); Tomaiuolo et al. (1999); www.bic.mni.mcgill.ca/software/Display/Display.html	Runs on Linux and SUN	Free	2D and 3D image viewing, ROI quantification (painting) on orthogonal sections in combination with lateral renderings, surface reconstruction	Knowledge of image orientation and gross neuroanatomy, depending on investigator's needs
Easymeasure	MARIARC, University of Liverpool, UK; Keller et al. (2007c); www.liv.ac.uk/mariarc	Runs on Windows only	Free	2D image viewing, stereological measurement	Knowledge of gross neuroanatomy for quantification
Freesurfer	Athinoula A. Martinos Center for Biomedical Imaging, Massachusetts, US; http://surfer.nmr.mgh.harvard.edu Articles: http://surfer.nmr.mgh.harvard.edu/fswiki/Articles	Runs on Linux or Mac OS	Free but FS-FAST component requires Matlab licence (www.mathworks.com)	2D and 3D image viewing, reformatting, brain extraction, tissue segmentation, spatial normalisation, cortical reconstruction, cortical inflation, flatmapping, ROI quantification	Depends on investigator needs. Most of segmentation and normalisation is automated, but ROI demarcation and quantification requires investigator expertise in neuroanatomy
FSL	Oxford Centre for Functional MRI of the Brain (FMRIB); www.fmrib.ox.ac.uk/fsl	Runs on Windows, Linux, Mac OS or SUN	Free	2D and 3D image viewing, reformatting, brain extraction, tissue segmentation, spatial normalisation, smoothing, stereotaxic template building, VBM	Similar to SPM
ImageJ	National Institutes of Health, US ; http://rsb.info.nih.gov/ij	Runs on Windows, Linux, or Mac OS	Free	2D and 3D image viewing, reformatting, enhancement, editing, basic measurements	Knowledge of image orientation and gross neuroanatomy, depending on investigator's needs
LowD	MARIARC, University of Liverpool, UK; Barrick et al. (2005); www.liv.ac.uk/mariarc	Runs on Linux and SUN	Free (although uses segmentation in SPM which requires a Matlab licence)	Automated cerebral hemisphere extraction and volume calculation, automated analysis of cerebral asymmetry	Method is a command line technique (e.g. batch-processing) and does not require MR image interaction

Appendix 1 **(continued)**

Software	Reference	Software and Hardware Compatibility	Cost	Functions	User Expertise
Measure	Centre for Imaging Science, John Hopkin's University, Maryland, US; Barta et al. (1997); http://cis.jhu.edu	Runs on Windows	Free	2D and 3D image viewing, reformatting, stereological and tracing measurements using orthogonal sections	Knowledge of image orientation and gross neuroanatomy for quantification
MIDAS	National Hospital for Neurology and Neurosurgery, Queen's Square, London, UK; Freeborough et al. (1997)	Runs on SUN	Free	2D and 3D image viewing, ROI quantification, brain segmentation, brain surface rendering, image registration	Neuroanatomical knowledge for ROI quantification, other computer automated processes available
MRIcro	Rorden and Brett (2000); www.sph.sc.edu/comd/rorden/mricro.html	Runs on Windows, Linux, on SUN	Free	2D and 3D image viewing, reformatting, skull stripping, surface reconstruction, ROI label creation	Knowledge of image orientation and gross neuroanatomy, depending on investigator's needs
NIH Image	National Institutes of Health, US; http://rsbweb.nih.gov/ij	Runs on Mac OS	Free	2D and 3D image viewing, reformatting, enhancement, editing, basic measurements	Knowledge of image orientation and gross neuroanatomy, depending on investigator's needs
NRIA	Brain Behavior Laboratory, University of Pennsylvania, USA; www.med.upenn.edu/bbl	Runs on SUN	Free	2D and 3D image viewing, reformatting, ROI quantification	Knowledge of image orientation and gross neuroanatomy, depending on investigator's needs
SEAL	Montreal Neurological Institute, McGill University, Canada; Caramanos et al. (1997); www.bic.mni.mcgill.ca/~georges/Seal_Reference/seal_howto.html	Runs on Linux and SUN	Free	Identifies sulcal patterns	Knowledge of sulcal morphology. Major sulci can be determined automatically
SPM	Wellcome Department of Imaging Neuroscience, University College London; www.fil.ion.ucl.ac.uk/spm	Runs on Windows, Linux, Mac OS or SUN	Free but requires Matlab (www.mathworks.com), price depends on license type.	2D and 3D image viewing, reformatting, brain extraction, tissue segmentation, spatial normalisation, smoothing, stereotaxic template building, voxel-based morphometry (VBM)	'Button pressing' interface, much of image interaction not necessary. VBM removes need for expert neuroanatomist. Understanding the use of Matlab language advantageous